

The dynamics of a memristor-based Rulkov neuron with fractional-order difference

Yan-Mei Lu(卢艳梅), Chun-Hua Wang(王春华), Quan-Li Deng(邓全利), and Cong Xu(徐聪)
Citation: Chin. Phys. B, 2022, 31 (**6**): 060502. DOI: 10.1088/1674-1056/ac539a
Journal homepage: http://cpb.iphy.ac.cn; http://iopscience.iop.org/cpb

What follows is a list of articles you may be interested in

Neural-mechanism-driven image block encryption algorithm incorporating a hyperchaotic system and cloud model

Peng-Fei Fang(方鹏飞), Han Liu(刘涵), Cheng-Mao Wu(吴成茂), and Min Liu(刘旻)
Chin. Phys. B, 2022, 31 (**4**): 040501. DOI: 10.1088/1674-1056/ac272d

A class of two-dimensional rational maps with self-excited and hidden attractors

Li-Ping Zhang(张丽萍), Yang Liu(刘洋), Zhou-Chao Wei(魏周超),Hai-Bo Jiang(姜海波), and Qin-Sheng Bi(毕勤胜)
Chin. Phys. B, 2022, 31 (**3**): 030503. DOI: 10.1088/1674-1056/ac4025

Cascade discrete memristive maps for enhancing chaos

Fang Yuan(袁方), Cheng-Jun Bai(柏承君), and Yu-Xia Li(李玉霞)
Chin. Phys. B, 2021, 30 (**12**): 120514. DOI: 10.1088/1674-1056/ac20c7

Controlling chaos and supressing chimeras in a fractional-order discrete phase-locked loop using impulse control

Karthikeyan Rajagopal, Anitha Karthikeyan, and Balamurali Ramakrishnan
Chin. Phys. B, 2021, 30 (**12**): 120512. DOI: 10.1088/1674-1056/ac1b83

A memristive map with coexisting chaos and hyperchaos

Sixiao Kong(孔思晓), Chunbiao Li(李春彪), Shaobo He(贺少波), Serdar Çiçek, and Qiang Lai(赖强)
Chin. Phys. B, 2021, 30 (**11**): 110502. DOI: 10.1088/1674-1056/abf4fb

---

SPECIAL TOPIC — Interdisciplinary physics: Complex network dynamics and emerging technology

The dynamics of a memristor-based Rulkov neuron with fractional-order difference

Yan-Mei Lu(卢艳梅), Chun-Hua Wang(王春华)†, Quan-Li Deng(邓全利), and Cong Xu(徐聪)

College of Computer Science and Electronic Engineering, Hunan University, Changsha 410082, *China*

(Received 7 December 2021; revised manuscript received 21 January 2022; accepted manuscript online 10 February 2022)

The exploration of the memristor model in the discrete domain is a fascinating hotspot. The electromagnetic induction on neurons has also begun to be simulated by some discrete memristors. However, most of the current investigations are based on the integer-order discrete memristor, and there are relatively few studies on the form of fractional order. In this paper, a new fractional-order discrete memristor model with prominent nonlinearity is constructed based on the Caputo fractional-order difference operator. Furthermore, the dynamical behaviors of the Rulkov neuron under electromagnetic radiation are simulated by introducing the proposed discrete memristor. The integer-order and fractional-order peculiarities of the system are analyzed through the bifurcation graph, the Lyapunov exponential spectrum, and the iterative graph. The results demonstrate that the fractional-order system has more abundant dynamics than the integer one, such as hyper-chaos, multi-stable and transient chaos. In addition, the complexity of the system in the fractional form is evaluated by the means of the spectral entropy complexity algorithm and consequences show that it is affected by the order of the fractional system. The feature of fractional difference lays the foundation for further research and application of the discrete memristor and the neuron map in the future.

Keywords: discrete memristor, Rulkov neuron, fractional-order difference, dynamics

PACS: 05.45.Ac, 05.45.–a, 87.19.ll, 05.45.Pq **DOI:** 10.1088/1674-1056/ac539a

1. Introduction

The biological nervous system contains many neurons, and changes in neuronal electrical activities affect the function of the nervous system. Particularly, electromagnetic radiation is generated owing to the extensive application of various electromagnetic communication instruments, and it is almost full of today's living environment. Due to the memristor can represent the electrical characteristics of the flux-charge domain, it can be applied to the neuron discharge model to study the influence of electromagnetic radiation on the electrical activities of neurons.[1–4] Compared with ordinary neuron models, memristor-based neurons can simulate the effects of electromagnetic radiation in the real environment, so they are closer to the actual biological neuron model. Experiments show that it can also bring more complex dynamics.

In the past decade, combined with memristors, many scholars have explored the dynamics of neurons and neural network systems under electromagnetic radiation. Compared with continuous-domain neurons (such as the famous HH model,[5] HR model,[6] *etc.*), the discrete domain (such as the classical Izhikevich model,[7] Rulkov model,[8] *etc.*) can simulate the firing behavior of neurons in a lower dimensionality and be used more effectively and accurately in real engineering applications.[9] Emulating electromagnetic radiation by discrete memristors on neuron maps is becoming an emerging research topic. Li *et al.* successfully implemented the discrete-memristor to simulate electromagnetic radiation on neurons for the first time in 2021.[10] However, their research is based on the form of integer order iteration maps. So far, no investigation on the dynamic behaviors of the memristor-based fractional Rulkov map has been found.

As the extension of integer order, fractional calculus is a vital branch of mathematics.[11] Owing to its memory characteristics and being closer to engineering reality,[12–15] it is extensively used in lots of fields.[16–19] In fact, as early as 1989, Miller and Ross began the study of discrete fractional difference and gave a preliminary definition.[20] But until recently, due to the important role of discrete dynamical systems in engineering, people began to pay attention to the research on the definition of discrete fractional order and achieved phased results.[21–25] However, the current research on fractional-order discrete chaotic systems is still in its infancy, and researches based on fractional-order discrete neurons is even rarer, requiring continuous exploration and research.

Based on the relationship between charge and magnetic flux, the memristor is a two-terminal electronic device proposed by Professor Leon Chua,[26] and a physical model was successfully developed by Hewlett Packard (HP) laboratory in 2008.[27] Due to its nanometer size, nonlinearity, and memory peculiarity, the memristor is widely used in chaotic circuits,[28,29] neural networks,[1,3] memory storage,[30,31] secure communications.[32,33] The concept of fractional memris-

†Corresponding author. E-mail: wch1227164@hnu.edu.cn

© 2022 Chinese Physical Society and IOP Publishing Ltd

tor was firstly proposed by Coopmans *et al.*[34] Since then, the fractional memristor has been closely watched by researchers. Unfortunately, there are relatively few studies on discrete fractional memristors. It is known that discrete memristors play an important role in the application of discrete systems. In our paper, a new fractional discrete memristor is constructed. Compared with the fractional memristor in Ref. [35], the modulus function of the new memristor has outstanding nonlinearity.

In summary, this paper proposes a new fractional-order discrete memristor model with superior non-linear features and constructs a memristor-based fractional Rulkov neuron map for the first time. The dynamics of the simple memristor-based map under integer order and fractional order are probed respectively. Simulation experiments demonstrate that the system can produce periodic and chaotic behaviors in integer-order form, but rich dynamic behaviors such as asymptotically periodic oscillation, hyper-chaos, multi-stable, and transient chaos appear in fractional-order form. Finally, the complexity of the fractional-order system is evaluated through the spectral entropy complexity algorithm. Results show that the complexity of the system is related to the fractional order.

The organization of the follow-up part of this article is as follows: The second part introduces the definition of discrete fractional-order difference. The third part constructs a new fractional-order discrete memristor model. The fourth part structure a two-dimensional Rulkov neuron mapping based on a discrete memristor and the dynamics of it are discussed in the form of integer order and fractional order, complexity is explored as well. Finally, the article is summarized.

2. The discrete fractional-order difference

Presently, the definition of fractional-order discrete system is mainly based on three types, Riemann–Liouville definition,[36] Caputo definition[22,36] and Grunwald–Letnokov definition.[37,38] Among them, the Riemann-Liouville difference equation needs to define the initial conditions, and the research on the Grunwald–Letnokov definition is relatively few, and many characteristics are not analyzed sufficiently. Relatively speaking, the Caputo definition not only does not have the problem of initial value definition but also has sufficient theoretical research and analysis, so the fractional difference operator in this article is based on it. In this part, we will introduce the Caputo definition firstly.

Define an independent time scalar $N_a = \{a, a+1, a+2, \ldots\}$, $a \in R$, and a discrete function as $x(n)$. The forward difference operator of this function is $\Delta x(n) = x(n+1) - x(n)$.

Definition 1[39] There is a relationship $f : N_a \to R$, then the score sum of order q ($q > 0$ is the fractional combination, $q < 0$ is the fractional difference) is defined as

$$\Delta_a^{-q} x(t) = \frac{1}{\Gamma(q)} \sum_{s=a}^{t-q} (t - \sigma(s))^{(q-1)} x(s), \tag{1}$$

among it, $t \in N_{a+q}$, a is the initial point, $\sigma(s) = s+1$. $\Gamma(\cdot)$ is the Gamma function, and $\Gamma(n) = \int_0^{+\infty} t^{n-1} \mathrm{e}^{-t} \mathrm{d}t$, $t^{(q)}$ is decreasing factorial factor and is defined as $t^{(q)} = \frac{\Gamma(t+1)}{\Gamma(t+1-q)}$.

Definition 2[36] When the fractional order $q > 0$, the Caputo difference operator is defined as

$$C\Delta_a^q x(t) = \frac{1}{\Gamma(m-q)} \sum_{s=a}^{t-(m-q)} (t - \sigma(s))^{(m-q-1)} \Delta_s^m x(s), \quad t \in N_{a+m-q}, \tag{2}$$

where a is the start point, and $m = \lceil q \rceil$.

Theorem 1[22] The Caputo fractional difference equation is defined as

$$\begin{aligned} &c\Delta_a^q x(t) = f(t+q-1, x(t+q-1)), \\ &\Delta^k x(a) = c_k, \quad k = 0, 1, \ldots, m-1. \end{aligned} \tag{3}$$

The definition can continue to be equivalent to the equation

$$\begin{aligned} x(t) = x(a) + \frac{1}{\Gamma(q)} &\sum_{s=a+m-q}^{t-q} (t - \sigma(s))^{(q-1)} \\ &\times f(s+q-1, x(s+q-1)). \end{aligned} \tag{4}$$

Furthermore, let $s + q = j$, then the equation can be changed to

$$x(t) = x(a) + \frac{1}{\Gamma(q)} \sum_{j=1}^{t} \frac{\Gamma(t-j+q)}{\Gamma(t-j+1)} f(j-1, x(j-1)). \tag{5}$$

According to Eq. (5), it can be observed that when the fractional order $q = 1$, this equation degenerates into a general integer-order difference equation. We can also see that the current moment is related to the value of all moments before it, which reflects the discrete memory effect of the fractional difference operator.

3. A new fractional discrete memristor

A continuous flux-controlled memristor model was proposed to simulate electromagnetic induction in Ref. [40]. The model was expressed as

$$\begin{cases} i = \tanh(\varphi) v, \\ \dot{\varphi} = v, \end{cases} \tag{6}$$

where i, v respectively represent the current flowing through the memristor and the voltage across it, and φ represents the internal state variable of the memristor. By imitating the continuous memristor discretization method of Ref. [41], the memristor model equation (6) was discretized, and a new discrete memristor model was constructed.[10] Variables i, v, φ were replaced by $i(n)$, $v(n)$, $\varphi(n)$ respectively, then the following discrete model could be obtained:

$$\begin{cases} i(n) = \tanh(\varphi(n)) v(n), \\ \varphi(n+1) = \varphi(n) + \varepsilon v(n), \end{cases} \tag{7}$$

where $\varphi(n+1)$ is the value of $\varphi(t)$ in the $(n+1)$-th iteration. The parameter ε represents the time scale factor of the induced electromotive force in a finite transient period, and it depends on the nature of the medium.

When the voltage applied across the memristor is $v(n) = H\sin(wn)$ (H is the amplitude, w is the frequency), let $H = 1$, figure 1 shows the volt-ampere curve of the discrete memristor. It is not difficult to see that the discrete memristor has three specialties of general memristor.[42]

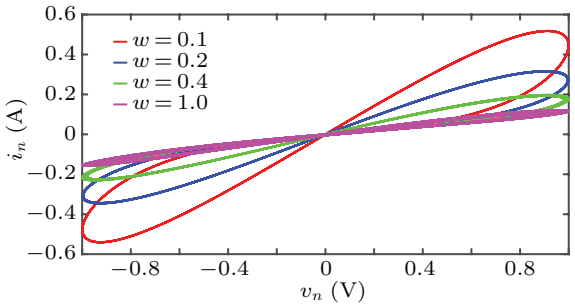


Fig. 1. The volt–ampere curve of the integer-order discrete memristor, $H = 1$.

In keeping with the definition of Caputo fractional difference in Part 2, the fractional form of the memristor can be described by the following equation:

$$\begin{cases} i(n) = \tanh(\varphi(n))v(n), \\ \varphi(n) = \varphi(0) + \dfrac{1}{\Gamma(q)}\displaystyle\sum_{j=1}^{n}\frac{\Gamma(n-j+q)}{\Gamma(n-j+1)}\varepsilon v(j-1). \end{cases} \tag{8}$$

It can be seen that the modulus function of the fractional discrete memristor is a hyperbolic tangent function with a nonlinear personality. This inherent nonlinearity is different from the traditional nonlinear characteristic outside the memristor, which makes the memristor have a more outstanding nonlinear feature. In addition, compared with the fractional memristor in Ref. [35], the modulus function of this new memristor is a single-valued nonlinear function with outstanding nonlinearity.

Let $H = 1$, $q = 0.65$, explore the relationship between the volt-ampere characteristics of the fractional discrete memristor and the input frequency. The results are shown in Fig. 2(a). Obviously, the area of the hysteresis sidelobe decreases as the frequency increases. It can be noticed that when $w = 3.0$, the relationship between the voltage across the memristor and the current through the memristor is approximately a single-valued function. This is consistent with the traits of the general memristor.

Setting $H = 1$, $w = 0.1$, figure 2(b) presents the correlation between the hysteresis loop of the discrete memristor and the fractional order q. It is easy to see that as the fractional order q increases, the area of the hysteresis sidelobe increases as well, indicating that the order q has an effect on the peculiarity of the discrete memristor, which is coincident with the conclusion of Ref. [35].

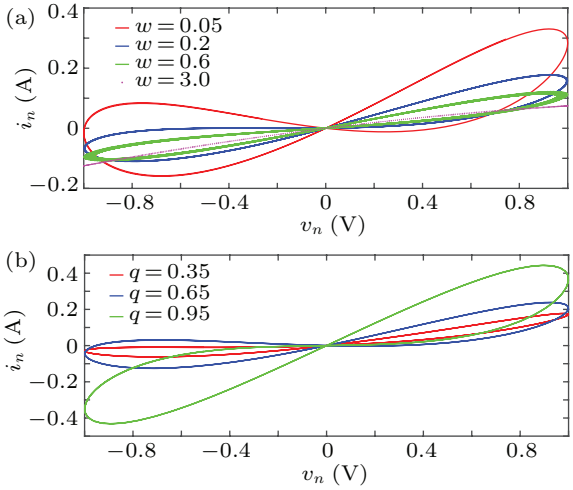


Fig. 2. The volt-ampere characteristic curve of the fractional discrete memristor. (a) $H = 1$, $q = 0.65$; (b) $H = 1$, $w = 0.1$.

4. The memristor-based Rulkov neuron with the fractional-order difference

4.1. The model of the fractional neuron map

In order to explore the characteristics of neurons more conveniently, researchers have proposed many neuron models based on experimental and theoretical analysis. In particular, the Rulkov neuron map is a typical discrete-domain neuron model. It is an abstract simple mathematical model, but it can represent the rich nonlinear dynamics and biological neuronal features.[43–45] Here, considering a one-dimensional map of Rulkov neuron[8]

$$x(n+1) = \frac{\alpha}{1+x(n)^2} + \beta. \tag{9}$$

This model can simulate the firing behaviors of a neuron, where the variable x represents the membrane potential of the neuron, and the variable β is relevant to the concentration of ions on the cell membrane.

The membrane potential of neurons is caused by the difference in the concentration of charged ions inside and outside the cell membrane. When neurons are stimulated by electromagnetic radiation, the moving charged ions will generate the electromagnetic induction current, thereby changing the membrane potential. Therefore, the influence of electromagnetic radiation on neurons can be equivalent to the induced current generated by external magnetic flux passing through the membrane potential.[1,4] Among them, the coupling of magnetic flux and membrane potential can be described by a flux-controlled memristor. Specifically, the discrete memristor represented by Eq. (7) can be used to characterize the induced current generated under the influence of electromagnetic radiation on the neuron described by Eq. (9). Hence, introducing Eq. (7) into the neuron described by Eq. (9), a new model is built as follows:

$$\begin{cases} x(n+1) = \frac{\alpha}{1+x(n)^2} + \beta + p\tanh(y(n))x(n), \\ y(n+1) = y(n) + \varepsilon x(n). \end{cases} \tag{10}$$

The Eq. (10) can imitate the dynamic behavior changes of the Rulkov neuron under electromagnetic radiation. Where $\tanh(y(n))x(n)$ means the induced current which is generated by electromagnetic induction, and the parameter p stands for the intensity of the induced current acting on the neuron. According to the Eq. (10), we can acquire the difference equation of the Rulkov neuron map based on the discrete memristor as

$$\begin{cases} \Delta x(n) = \dfrac{\alpha}{1+x(n)^2} + \beta + p\tanh(y(n))x(n) - x(n), \\ \Delta y(n) = \varepsilon x(n). \end{cases} \tag{11}$$

Similarly, the Caputo fractional difference operator is imported into the above formula to obtain the fractional form of the discrete map. As shown in the following

$$\begin{cases} x(n) = x(0) + \dfrac{1}{\Gamma(q)}\sum_{j=1}^{n}\dfrac{\Gamma(n-j+q)}{\Gamma(n-j+1)} \\ \qquad \left[\dfrac{\alpha}{1+x(j-1)^2} + \beta \right. \\ \qquad \left. + p\tanh(y(j-1))x(j-1) - x(j-1)\right], \\ y(n) = y(0) + \dfrac{1}{\Gamma(q)}\sum_{j=1}^{n}\dfrac{\Gamma(n-j+q)}{\Gamma(n-j+1)}\left[\varepsilon x(j-1)\right], \end{cases} \tag{12}$$

where $x(0)$ stands for the initial membrane potential of the neuron, and $y(0)$ represents the initial voltage across the memristor. It can be seen from the Eq. (12) that due to the influence of the fractional-order difference operator, the current mode voltage of the neuron is related to the past moments. It reflects the property of memory and corresponds to the memory nature of the organism itself, so this model is more practical.

4.2. The dynamics of the fractional neuron map

In the process of studying and observing system dynamics, some specific methods are needed to describe the characteristics of the system clearly and intuitively. Here are three types used in this article:[46]

(i) Iteration diagram: It is the record of the movement track of one dimensional, you can directly observe the position of the system in a certain iteration, which is the most direct way to observe the movement state of the system.

(ii) Bifurcation diagram: When the system parameter changes, the projection of the trajectory of the system on a certain coordinate axis can constitute the bifurcation diagram. When the system is in a periodic state, the bifurcation graph appears as periodic points, and when the system is in a chaotic state, the bifurcation graph appears as irregularly distributed points.

(iii) Lyapunov exponent: It can characterize the characteristics of system motion. The positive and negative values of the Lyapunov exponent in a given direction represent the average speed of divergence or convergence of adjacent orbits in the attractor in that direction over a period of time. When the maximum Lyapunov of the system is equal to zero, the system is in a periodic state. When the system has only one Lyapunov exponent greater than zero, the system is in a chaotic state. When the system has two or more Lyapunov exponents greater than zero, the system is in a hyperchaotic state.

Next, the dynamic behaviors of the Rulkov neuron map based on the discrete memristor in fractional-order will be explored. Before researching the fractional-order characteristics of the system, let's take a look at the dynamics of the integer-order system. For Eq. (10) when $\alpha = 4.1$, $p = 0.5$, $\varepsilon = 0.04$, $x(0) = -0.3$, $y(0) = 0.2$ are fixed, the bifurcation diagram and the Lyapunov exponential spectrum are used to investigate the change of system dynamics with the parameter β. The bifurcation diagram is shown in Fig. 3(a). It can be seen that the system starts from the periodic states and gradually enters into the chaotic states by the period-doubling bifurcation. Then there is the phenomenon of alternating periods and chaotic states, finally returning to the periodic states through the reverse period-doubling bifurcation. In Fig. 3(b), changes in the value of the Lyapunov exponents are consistent with the bifurcation diagram. It can be observed that in the whole change process, there is at most one Lyapunov exponent greater than zero, which shows that the system does not appear in hyperchaotic states.

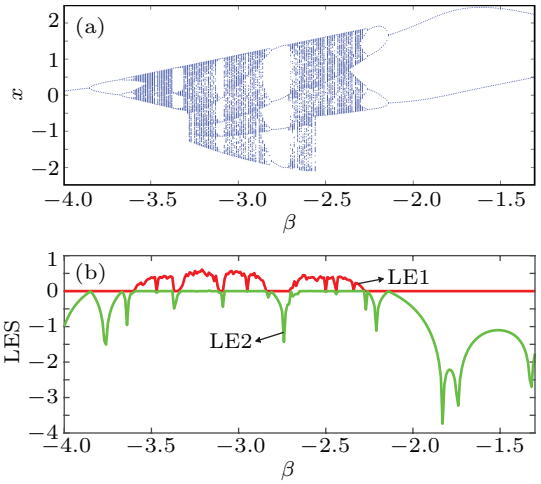


Fig. 3. The dynamics of the system in the integer order: (a) the bifurcation diagram; (b) the Lyapunov exponential spectrum.

4.2.1. Asymptotically periodic oscillations

Unlike the integer-order systems, there are no exact periodic solutions in the fractional-order one.[47] However, through Ref. [48], we can know that there are asymptotically periodic characteristics in some fractional systems.

Theorem 2[49] For the given fractional difference equation

$$\begin{aligned} D^q x_i(t) &= f_i(x_1(t), x_2(t), \ldots, x_n(t)), \\ & i = 1, 2, \ldots, n, \quad 0 < q < 1, \end{aligned} \tag{13}$$

when the trajectory of the system shown in Eq. (13) satisfies $\lim_{n\to\infty} x_i(t+T) - x_i(t) = 0$, $i = 1, 2, \ldots, n$ and $T > 0$, it is named

"asymptotically T-periodic oscillations". In the new fractional map proposed in our article, this behavior also exists. For example, setting parameters $\alpha = 5$, $\beta = -3$, $p = 0.5$, $\varepsilon = 0.04$, $q = 0.75$ and parameters $\alpha = 3.9$, $\beta = -2.5$, $q = 0.65$ respectively, Fig. 4 presents the corresponding iteration diagrams under the initial state $x(0) = 3.5$, $y(0) = -1.5$. From Fig. 4(a), we know $\lim_{n\to tn} x_i(n+T) - x_i(n) = 0$, $i = 1,2,\ldots$, $T > 0$, and from Fig. 4(b), we know $\lim_{n\to tm} x_i(n+T) - x_i(n) = 0$, $i = 1,2,\ldots$, $T > 0$. Obviously, they are all asymptotically periodic oscillations. It is worth noting that the periodic behaviors of the fractional-order system in the following text are all asymptotic periodic oscillations. For convenience, we simplify the "asymptotic periodic oscillations" to "A–P–O".

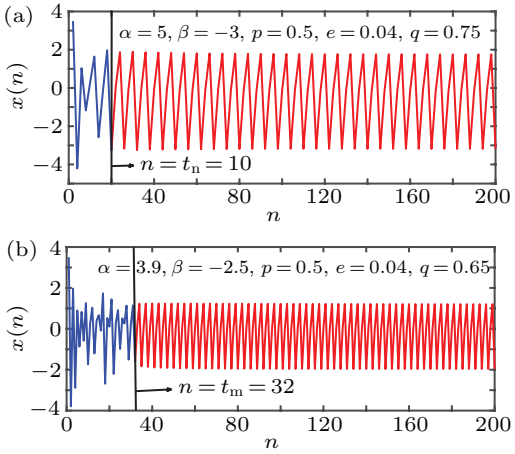


Fig. 4. The asymptotically periodic oscillations of the fractional neuron map under the initial state $x(0) = 3.5$, $y(0) = -1.5$.

4.2.2. The hyperchaotic property of the fractional neuron map

Likewise, the dynamics of the fractional-order system Eq. (12) are searched by the bifurcation diagram and Lyapunov exponential spectrum as well. For the Lyapunov exponents of fractional discrete chaotic systems, there are only two methods: one is the Jacobian matrix method[50] and the other is the Wolf algorithm.[51] The calculation speed of the Wolf algorithm is relatively slow, so the Jacobian matrix method is adopted in this article. Special attention should be paid to the use of this method in fractional systems. The detailed process can be found in Ref. [52].

Compared with integer order form, when the fractional order $q = 0.85$ and other conditions $\alpha = 4.1$, $p = 0.5$, $\varepsilon = 0.04$ remain unchanged, the simulation results are shown in Fig. 5(a). Here, we draw the bifurcation diagram and the Lyapunov exponential spectrum together. It is helpful to observe whether the two changes are synchronized. Obviously, with the change of variable β, the system appears A–P–O and hyperchaos. For example, when $\beta = -3.99$ and $\beta = -3.8$, the system is in one asymptotically periodic oscillations and two asymptotically periodic oscillations respectively, and it behaves as hyperchaotic behavior when $\beta = -3.2$. The iteration diagrams are shown in Figs. 5(b)–5(d). The appearance of the hyperchaotic states indicates that the fractional-order form of the system has more complex dynamics than the integer-order.

In order to explore the impact of the fractional order on the system, in the following content, the dynamic performance of the system at different orders will be probed. As shown in Figs. 6(a)–6(d), under certain other conditions, the bifurcation diagrams and Lyapunov exponential spectrums corresponding to the different q are significantly different, which means diverse dynamic behaviors. But the same is that all cases possess hyperchaotic behavior changes. Since there are at least two Lyapunov exponents greater than zero, the hyperchaotic state[53] of the chaotic system has more complex behavior, and the generated sequence is closer to the pseudo-random sequence. Applying it to the field of secure communication, the system will have stronger anti-interference and anti-interception capabilities, and the security effect will be better.

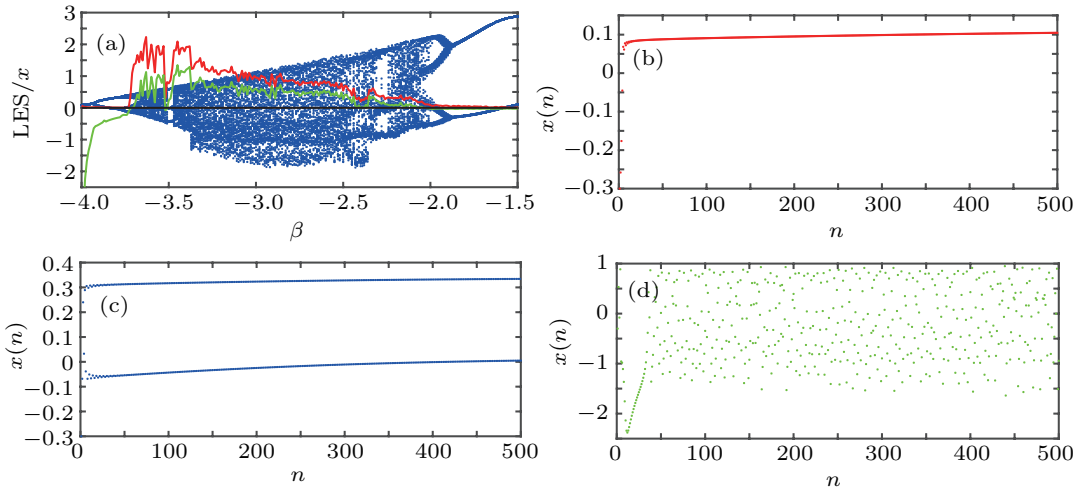


Fig. 5. The dynamics of the fractional system with the parameters $\alpha = 4.1$, $p = 0.5$, $\varepsilon = 0.04$, $q = 0.85$. (a) The bifurcation diagram and the Lyapunov exponential spectrum. (b) Iterative graph at $\beta = -3.99$. (c) Iterative graph at $\beta = -3.8$. (d) Iterative graph $\beta = -3.2$.

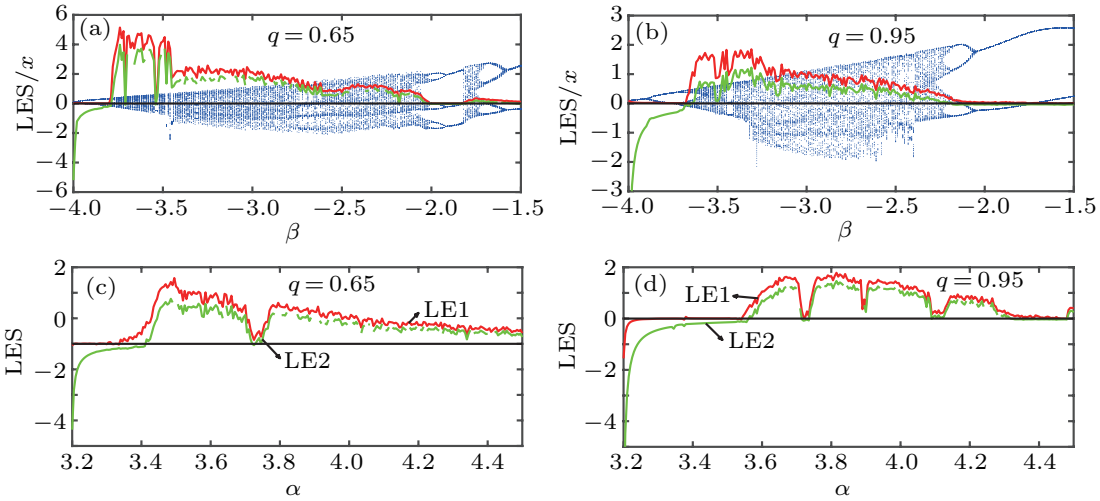


Fig. 6. The effect of fractional order q on system dynamics. (a) The bifurcation diagram of $\beta, q = 0.65$. (b) The bifurcation diagram of $\beta, q = 0.95$. (c) The Lyapunov exponential spectrum of $\alpha, q = 0.65$. (d) The Lyapunov exponential spectrum of $\alpha, q = 0.95$.

4.2.3. The multistability of the fractional neuron map

The multistability[54] of a chaotic system means that when other parameters other than the initial value remain unchanged, the system displays three or more coexisting states. It is an important manifestation of the influence of the chaotic system on the initial values.

When the system parameters $\alpha = 3.9$, $p = 0.5$, $\varepsilon = 0.04$, and $q = 0.65$ are settled, different initial values are chosen to verify the multi-stable behavior of the fractional-order system Eq. (12). Figure 7(a) shows the simulation results. Among it, the initial values of the red dot graphs are (3.5, −1.5), the green dot graphs represent the initial values of (0.1, 0.1), and the initial values of the blue one are (−7, −0.01). It can be seen that the red, green, and blue in the figure appear intermittently in some areas. When the same parameters are selected, the system exhibits different behaviors, which signifies the multi-stable coexistence. For example, when $\beta = -3.7$, the two asymptotically periodic oscillations (green), the chaotic state (red), and the one asymptotically periodic oscillations (blue) are shown respectively; when $\beta = -3.3$, the behaviors under the three different initial conditions are also different. The specific iteration diagrams are presented in Figs. 8(a) and 8(b).

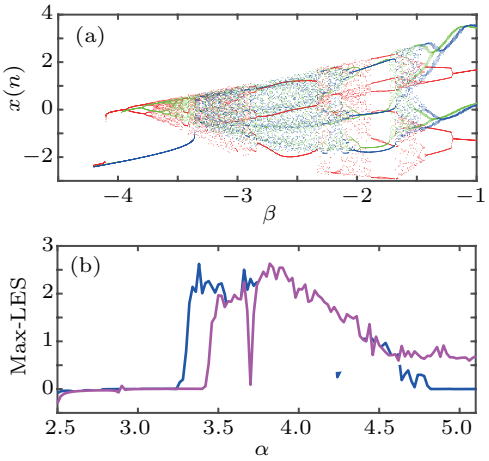


Fig. 7. The multistability of the fractional-order system. (a) The bifurcation diagram of the system with different initial values, red (3.5, −1.5), green (0.1, 0.1), blue (−7, −0.01). (b) The max Lyapunov exponent spectrum of the system with different initial values, blue (3.5, −1.5), purple (0.1, 0.1).

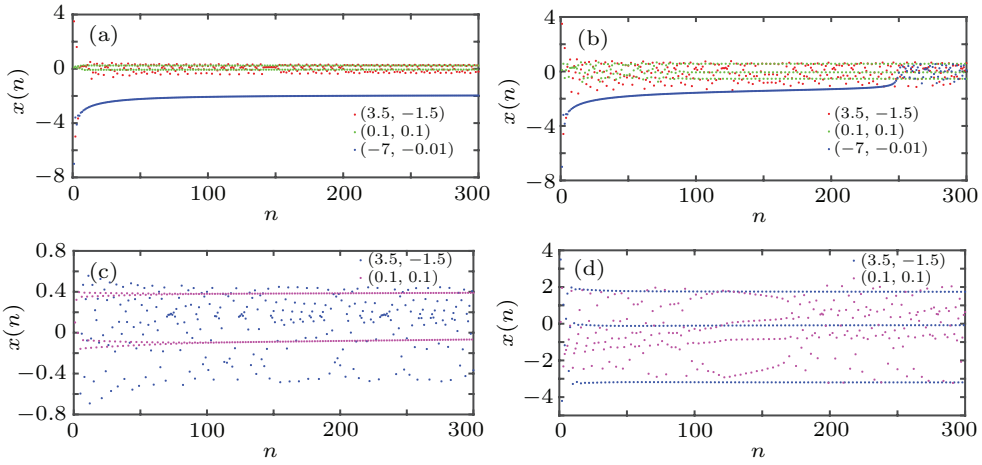


Fig. 8. The multistability iterative graphs of the fractional system. (a) $\beta = -3.7$, $q = 0.65$; (b) $\beta = -3.3$, $q = 0.65$; (c) $\alpha = 3.35$, $q = 0.75$; (d) $\alpha = 5$, $q = 0.75$.

Furthermore, the coexistence of different states in the system is confirmed by the largest Lyapunov exponential spectrum. Setting $\beta = -3$, $p = 0.5$, $\varepsilon = 0.04$, $q = 0.75$, figure 7(b) shows the maximum Lyapunov exponents under the initial values (3.5, −1.5) (blue) and (0.1, 0.1) (purple). Apparently, the system has coexisting attractors. Figures 8(c) and 8(d) give two specific examples. When $\alpha = 3.35$, the system presents two asymptotically periodic oscillations (purple) and chaotic state (blue) respectively under two initial values. When $\alpha = 5$, three asymptotically periodic oscillations (blue) and a chaotic state (purple) can get under the initial values (3.5, −1.5) and (0.1, 0.1).

4.2.4. The transient chaos of the fractional neuron map

In some continuous systems, there is a phenomenon of transient chaos.[55] Similarly, in a discrete system, the phenomenon of transient chaotic behavior means that the nonlinear system appears a chaotic sequence in a finite iteration interval, then evolves into a period or another hyperchaotic/chaotic state with the number of iterations. But there are few reports in the discrete system.

In the fractional discrete map constructed in this paper, under certain initial conditions and parameters, different transient chaotic phenomena appear. Figure 9 shows three specific examples, where figure 9(a) shows the result of the iteration when the parameters $\alpha = 4.1$, $\beta = -2.1$, $p = 0.5$, $\varepsilon = 0.04$, $q = 0.65$, and the initial conditions are (0.1, 0.1). It can be found that when the number of iterations n is less than 400, the system is in a chaotic state, evolving from $n = 400$ to an A–P–O state. Figure 9(b) is the result of the iteration under the same condition as (a) and $q = 0.75$. It is not difficult to find that the system is in a chaotic state at the beginning of the iteration, but when $n = 240$, it begins to enter into an A–P–O state. When $n = 435$, the system begins to enter the chaotic state again. Yet, let $\alpha = 3.9$, $\beta = -1.7$, $p = 0.5$, $\varepsilon = 0.04$, $q = 0.65$, the iterative simulation diagram is shown in Fig. 9(c). Vividly, as the iteration progresses, the system goes through the A–P–O, chaos, and A–P–O in turn. In summary, we can conclude that there are abundant transient chaotic behaviors in this fractional-order system.

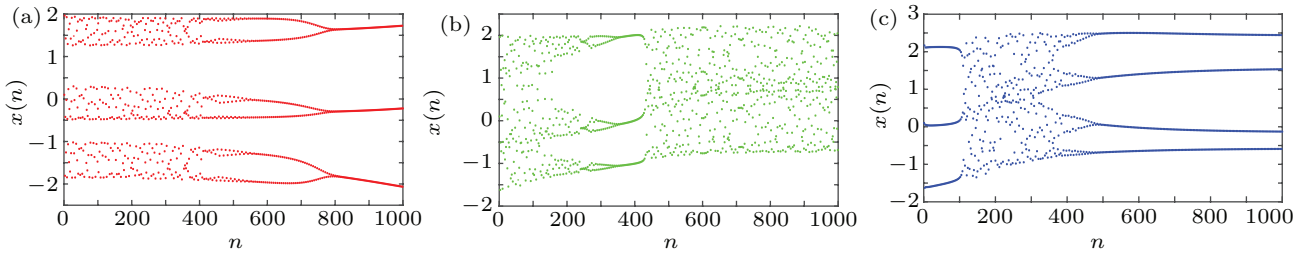


Fig. 9. The transient chaos iterative graphs of the fractional system. (a) $\alpha = 4.1$, $\beta = -2.1$, $q = 0.65$; (b) $\alpha = 4.1$, $\beta = -2.1$, $q = 0.75$; (c) $\alpha = 3.9$, $\beta = -1.7$, $q = 0.65$.

4.3. The complexity of the fractional neuron map

The chaotic pseudo-random sequence has similar randomness, so it has a broad range of application prospects in the field of encryption and secure communication. The complexity can be used to measure the closeness between the chaotic pseudo-random sequence and the real random sequence. The higher the complexity, the closer to the random sequence, the stronger the system's anti-interference and anti-interception capacity, and the better communication security effect. Therefore, it is meaningful to investigate the complexity of chaotic systems.

The complexity of chaotic systems can be analyzed from two aspects: behavior and structure. The main concern in this article is the latter. Structural complexity refers to the analysis of sequence complexity through frequency characteristics and energy spectrum characteristics in the transform domain. The more balanced the energy spectrum distribution in the sequence transform domain, the closer the sequence is to a random signal. To analyze the complexity of the chaotic pseudo-random sequence generated by the fractional mapping Eq. (12), the spectral entropy (SE) complexity algorithm[56] based on the Fourier transform is utilized.

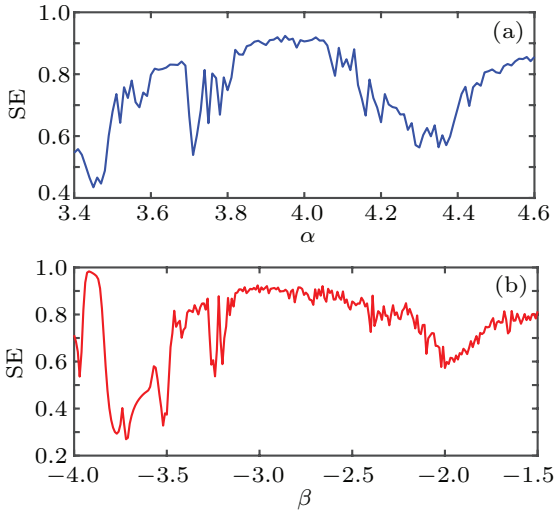


Fig. 10. The variation of complexity with the parameters α, β.

Figure 10 shows the impact of system parameter variation on the system complexity when $\beta = -3$, $q = 0.85$ and $\alpha = 3.9$, $q = 0.85$ separately. It can be observed that the size of the SE

complexity continuously fluctuates with the change of the parameter, which illustrates the influence of the parameter on the system complexity.

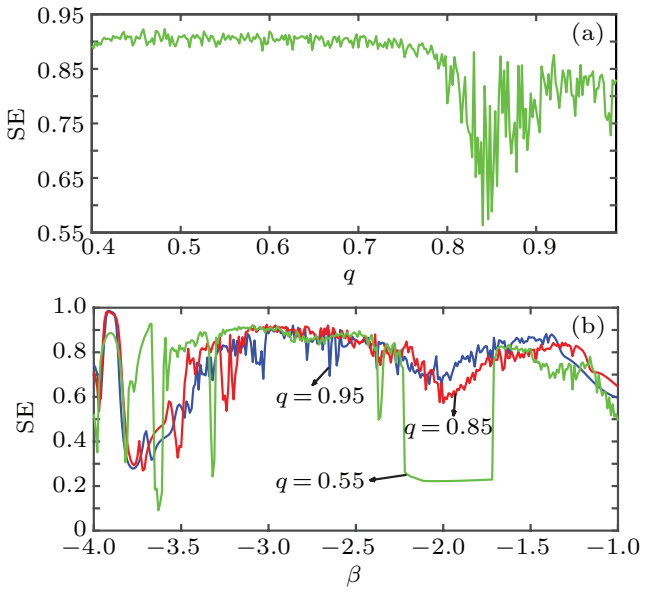


Fig. 11. The variation of complexity with fractional order q.

In addition, the influence of fractional order on sequence complexity is also inspected. Figure 11 specifically shows how the sequence complexity changes with the fractional order q. It can be seen that with the diversification of the fractional order, the value of SE changes non-directionally and fluctuates up and down, symbolizing that the order q can affect the complexity of the system and then affect the application effect of the system.

5. Conclusion and perspectives

In this paper, we construct a fractional discrete memristor with remarkable single-valued nonlinearity firstly, then propose a straightforward two-order map by coupling a discrete memristor with a one-dimensional Rulkov neuron map. Integer-order and fractional-order dynamic traits of the system are investigated respectively. Numerical simulation results show that the fractional form of the system has richer dynamics and higher complexity. It can be acquired that the application of fractional-order difference in discrete neuron maps based on the memristor can not only better simulate the fractional characteristics of biological neurons, but also bring more intricate dynamics. The peculiarities of fractional-order difference lay the foundation for further research and application of discrete neuron map in the future. In the next work, we will deeply study the fractional-order specialties of the discrete neuron networks under the action of the memristor.

Acknowledgements

Project supported by the Major Research Plan of the National Natural Science Foundation of China (Grant No. 91964108), the National Natural Science Foundation of China (Grant No. 61971185), and the Natural Science Foundation of Hunan Province, China (Grant No. 2020JJ4218).

References

[1] Lin H R and Wang C H 2020 *Appl. Math. Comput.* **369** 124840
[2] LV M and Ma J 2016 *Neurocomputing* **205** 375
[3] Lin H R, Wang C H, Hong Q H and Sun Y C 2020 *IEEE Transactions on Circuits and Systems II: Express Briefs* **67** 3472
[4] Lin H R, Wang C H, Chen C J, Sun Y C, Xu C and Hong Q H 2021 *IEEE Transactions on Circuits and Systems I: Regular Papers* **68** 3397
[5] Hodgkin A L and Huxley A F 1990 *Bull. Math. Bio.* **52** 25
[6] Hindmarsh J and Rose R M 1984 *Proceedings of the Royal Society of London. Series B, Biological Sciences* **221** 87
[7] Izhikevich and E M 2003 *IEEE Trans. Neural Networks* **14** 1569
[8] Rulkov N F 2001 *Phys. Rev. Lett.* **86** 183
[9] Bao H, Hua Z Y, Li H Z, Chen M and Bao B C 2021 *IEEE Transactions on Circuits and Systems I: Regular Papers* **68** 4534
[10] Li K X, Bao H, Li H Z, Ma J, Hua Z Y and Bao B C 2021 *IEEE Transactions on Industrial Informatics* PP 1
[11] Hilfer R 2000 *World Scientific Computer Sci.* **463** 472
[12] Petras I 2010 *IEEE Transactions on Circuits and Systems II-Express Briefs* **57** 975
[13] Ahmad W M and Sprott J C 2003 *Chaos, Solitons & Fractals* **16** 339
[14] Lu J G and Chen G R 2006 *Chaos, Solitons & Fractals* **27** 685
[15] Dong J, Zhang G J, Xie Y, Yao H and Wang J 2014 *Cognitive Neurodynamics* **8** 167
[16] Wei Y H 2021 *Nonlinear Dynamics* **104** 3643
[17] Yang N N, Han Y C, Wu C J, Jia R and Liu C X 2017 *Chin. Phys. B* **26** 080503
[18] Xie W L, Wang C H and Lin H R 2021 *Nonlinear Dynamics* **104** 4523
[19] Li R G and Wu H N 2019 *Nonlinear Dynamics* **95** 1221
[20] Miller K S and Ross B 1989 *Proceedings of the International Symposium on Univalent Functions, Fractional Calculus and Their Applications* 139–152
[21] Edelman M 2012 *Discontinuity, Nonlinearity and Complexity* **1** 305
[22] Edelman M 2015 *Discontinuity, Nonlinearity and Complexity* **4** 391
[23] Khennaoui A A, Quannas A, Bendoukha S, Wang X and Pham V T 2018 *Entropy* **20** 530
[24] Liu Z Y, Xia T C and Wang J B 2018 *Chin. Phys. B* **27** 030502
[25] Peng Y X, Sun K H, He S B and Peng D 2019 *Entropy* **21** 27
[26] Chua L 1971 *IEEE Trans. Circuit Theory* **18** 507
[27] Strukov D B, Snider G S, Stewart D R and Williams R S 2008 *Nature* **453** 80
[28] Yang Z L, Liang D, Ding D W, Hu Y B and Li H 2021 *Chin. Phys. B* **30** 120515
[29] Zhou L, Wang C H and Zhou L L 2018 *International Journal of Circuit Theory and Applications* **46** 84
[30] Guo M, Liu R Y, Dou M L and Dou G 2021 *Chin. Phys. B* **30** 068402
[31] Yang L M and Wang C H 2021 *Neurocomputing* **460** 117
[32] Cheng G F, Wang C H and Xu C 2020 *Multimedia Tools and Applications* **79** 29243
[33] Chai X L, Gan Z H, Lu Y, Zhang M H and Chen Y R 2016 *Chin. Phys. B* **25** 100503
[34] Coopmans C, Pet I and Chen Y Q 2009 *ASME 2009 International Design Engineering Technical Conferences and Computers and Information in Engineering Conference*, August 2, 2009, San Diego, USA
[35] Peng Y X, He S B and Sun K H 2021 *Results in Physics* **24** 104106
[36] Abdeljawad T 2011 *Comput. Math. Appl.* **62** 1602
[37] Nosrati K and Shafiee M 2018 *Chaos, Solitons & Fractals* **115** 224
[38] Ji Y D, Lai L and Zhou S C 2017 *Commun. Nonlinear Sci. Numer. Simul.* **57** 352
[39] Atici F and Eloe P W 2009 *Proc. Am. Math. Soc.* **137** 981
[40] Bao H, Hu A H, Liu W B and Bao B C 2019 *IEEE Transactions on Neural Net-works and Learning Systems* **31** 502
[41] Li H Z, Hua Z Y, Bao H, Zhu L, Chen M and Bao B C 2021 *IEEE Transactions on Industrial Electronics* **68** 9931

[42] Adhikari S P, Sah M, Kim H and Chua L 2013 *IEEE Transactions on Circuits & Systems. Part I: Regular Papers* **60** 3008
[43] Rajasekar S, Used J and Wagemakers A 2012 *Commun. Nonlinear Sci. Numer. Simul.* **17** 3435
[44] Wang, C X and Cao H J 2014 *Commun. Nonlinear Sci. Numer. Simul.* **20** 536
[45] Irina Bashkirtseva 2015 *Discrete Dynamics in Nature & Society* **2015** 1
[46] Yu S M 2011 *Chaotic systems and chaotic circuits:principle, design and its appliction in communications* (Xi'an: Xidian University Press) pp. 10–58
[47] Eva K and Seenith S 2012 *Nonlinear Analysis: Real World Applications* **13** 1489
[48] Kang Y M, Xie Y, Lu J C and Jiang J 2015 *Nonlinear Dynamics* **82** 1259
[49] Danca M F, Feckan M, Kuznetsov N V and Chen G R 2018 *Nonlinear Dynamics* **91** 2523
[50] Wu G C and Baleanu D 2015 *Commun. Nonlinear Sci. Numeri. Simul.* **22** 95
[51] Wolf A, Swift J, Harry L S and Vastano J 1985 *Physica D* **16** 285
[52] Ouannas A, Khennaoui A A, Wang X, Pham V T, Boulaaras S and Momani S 2020 *The European Physical Journal Special Topics* **229** 2261
[53] Yu F, Qian S, Chen X, Huang Y Y, Liu L, Shi C Q, Cai S, Song Y and Wang C H 2020 *Int. J. Bifurc. Chaos* **30** 2050147
[54] Lin H R, Wang C H, Deng Q L, Xu C, Deng Z K and Zhou C 2021 *Nonlinear Dynamics* **106** 959
[55] Celso G, Edward O and James A Y 1986 *Phys. Rev. Lett.* **57** 1284
[56] Sun K H, He S B, He Y and Yin L Z 2013 *Acta Phys. Sin.* **62** 010501 (in Chinese)